An Experimental Investigation of a Three-Dimensional Wall Jet

G.D. Catalano,* J.B. Morton,† and R.R. Humphris‡
University of Virginia, Charlottesville, Va.

An experimental investigation of the effects of a curved and flat wall surface on the flow development of an axisymmetric jet exhausting into a moving airstream has been made. Of primary concern was the comparison of the one-point statistical properties of the unconfined jet to the quantities measured in the flows over a flat plate and a curved wall surface. Quantities measured in this investigation included mean velocities in all three directions, turbulent intensities, autocorrelations, power spectral densities, and intermittencies. The investigation was confined to the near field of the turbulent jet. The curved wall (flap) was found to have a very large effect on both the mean velocity and the turbulent velocity components of the flowfield. The potential core region of the jet was found to break up most rapidly for the flow over the flap. A laser-Doppler velocimeter, using a phase locked-loop processor, was used to make the desired velocity field measurements. To determine the intermittency profiles, a laser light scattering technique was employed.

Nomenclature

D = diameter of nozzle
f = frequency of fluctuations
F = spectral density
I = intermittency
L = distance from bottom of test section
r_0 = radius of nozzle
R = autocorrelation coefficient
$R_{uu'}$ = two-point correlation coefficient
t = time
Δt = increment in time
u = velocity fluctuations in longitudinal direction
U = mean velocity in longitudinal direction
U = mean velocity in longitudinal direction
U^* = mean velocity at a given location in the flowfield parallel to surface of the flap
U_{FS} = freestream mean velocity
U_0 = maximum mean velocity of jet at exit plane
v = velocity fluctuations in lateral direction
V = mean velocity in lateral direction
W = mean velocity in vertical direction
x = downstream distance from exit plane of jet
y = lateral distance from centerline of jet/flap assembly
z = vertical distance above upper surface of flap
η = perpendicular height above surface of curved wall surface
$| \ |$ = absolute value of quantity
$(\overline{\ })$ = mean value of quantity

I. Introduction

In a previous study[1] an experimental investigation of the flow development of an axisymmetric jet exhausting into a moving airstream was made. Detailed mappings of one-point statistical properties such as mean velocities, turbulent intensities, and intermittencies were made between zero and eight diameters downstream from the jet exit plane. Also, autocorrelation and power spectral density curves were obtained for both the fluctuating velocity field and the concentration signal.

The purpose of this investigation was to determine the effects of wall surfaces with different radii of curvature on the flowfield of the axisymmetric jet. The positioning of the different surfaces relative to the exit plane of the jet (Fig. 1) corresponds to the upper surface blowing (USB) technique which presently is being proposed as a possible approach in attempting to increase the short takeoff and landing capability of aircraft.[2] Of primary concern in this investigation is the comparison of one-point statistical properties measured at the same position in the flowfield relative to the exit plane of the jet, with and without the wall structures present. Figure 2 indicates the positioning of the wall surfaces as well as the coordinate system used in this report.

As in the unconfined jet, in a wall jet there exists two main zones of flow: 1) an initial zone of flow establishment which consists of the growth of the boundary layer on the wall, the potential core, and the mixing region where the flow mechanism is similar to that of a free boundary jet problem, and 2) a zone of established flow which can be subdivided into a region of free mixing, where the flow condition and mixing process are similar to a free boundary jet, and the inner layer which is a class of boundary layer under a turbulent decelerating superstream.[3]

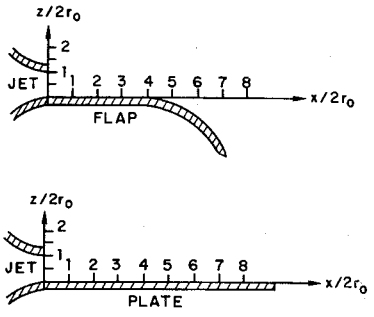

Fig. 1 Flow configurations.

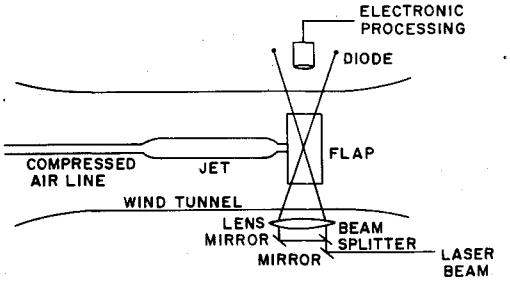

Fig. 2 Schematic of laboratory setup.

Received Dec. 13, 1976; revision received April 25, 1977.
Index category: Jets, Wakes, and Viscid-Inviscid Flow Interactions.

*Graduate student, Department of Engineering Science and Systems.
†Associate Professor, Department of Engineering Science and Systems. Member AIAA.
‡Senior Scientist, Department of Engineering Science and Systems.

The two-dimensional wall jet first was investigated by Forthman[4] in 1936. Glauert,[5] Schwarz and Cosart,[6] Sigalla,[7] and Myer et al.[8] added theoretical background and analysis to the problem. It was found that the velocity profiles, excluding the viscous sublayer near the wall, were similar. Mura Hari[3] proposed analytical methods for predicting the flow development region and the bed shear distribution in a wall jet. Dvorak[9] determined an analytical method for turbulent boundary layers and wall jets in which the effects of large longitudinal surface curvature and the associated normal pressure gradients were included for the first time. The Reynolds stress terms in the equation of motion were approximated using an eddy viscosity approach based on the concept of intermittency. Blackwelder and Kovasznay[10] obtained space-time correlations with large streamwise separation in a turbulent boundary layer with a zero-pressure gradient. The use of conditional averaging techniques led to an average picture of the velocities in the interfacial bulges.

The three-dimensional turbulent wall jet was investigated by Rajaratnam and Pani.[11] Experimental observations on the velocity and length scales and wall shear stress for wall jets issuing from circular, square, triangular, and elliptic nozzles were presented. It was found that the length scale in transverse direction grew about five times as fast as the length scale in the vertical direction. Narain[12] analytically investigated three-dimensional flows and found that the maximum velocity shows three regions of decay. The potential core region is followed by a region where the velocity decay is dependent on the shape and aspect ratio of the orifice. Following this region is a radial wall-jet-type maximum velocity decay region. Hill[13] looked at the effect of confining walls on a coflowing turbulent jet. It was shown that, before the jet spreads to the wall, both the mean velocity and turbulent shear stress are self-preserving. Afterwards, only the shear stress is subject to this condition.

II. Experimental Equipment and Techniques

The flow system[1] consists of a jet whose compressed air is marked with dioctyl phthalate (DOP) mounted inside the test section of a low-turbulence-level subsonic wind tunnel. With the parallel secondary flow in the wind tunnel being kept at a constant speed of 3.20 m/sec, the ratio of the exit plane velocity of the jet (16.30 m/sec) to the velocity of the tunnel air, (λ_j), is 5.1:1. The jet nozzle has a contraction ratio of 14 to 1 over a length of 15.9 cm. The Reynolds number of the jet flow is 22,600 using the nozzle diameter ($2r_0 = 2.14$ cm) as the length scale.

The curved wall surface (henceforth denoted "flap") is composed of two sections, a flat surface 17.80 cm wide and 7.50 cm long and a curved portion with a radius of curvature of 6.50 cm and sweeping out an arc of 70 deg. As has been mentioned previously, the flap is a scaled down model of an actual aerofoil surface presently being used in an USB investigation at NASA-Langley.[2] The ratio of the dimensions of full-scale configuration to the model used in this investigation is approximately 12 to 1. It also should be mentioned that great care was exercised in insuring a smooth transition between the inner surface of the jet and the upper surface of the flap.

Along with the investigation of a lifting device in a wind tunnel comes the need to check for separation from the nozzle and the trailing edge of the flap. Also the uniformness of slower moving secondary flow outside the jet's velocity field must be investigated.

A static pressure probe connected to a ⅛-in. condenser-type microphone was traversed along the outside of the contraction section of the jet nozzle and also along the surface of the flap. No evidence of separation from either the jet nozzle or flap was found. Total pressure surveys in the x direction were taken with traversing in the direction perpendicular to the level surface of the flap. Four such surveys are presented in Fig. 3, and they show that the outer tunnel flow is still relatively uniform. It should be noted that in comparing the total pressure measurements to the LDV data, the LDV system produces conditionally sampled information.

The flat wall surface (henceforth denoted "plate") is 30.50 cm long. For this configuration, as well, care was exercised in insuring a smooth transition between the jet and the upper surface of the plate. By examining the statistical properties of the flow over the plate, it is hoped that the effects of the curvature of the flap can be determined more clearly. The leading edge of both the flap and plate were contoured to provide as small a disturbance as possible to the tunnel flow. Flow visualization (using DOP) as well as a pressure probe/microphone listening technique indicated a smooth transition by the outer tunnel flow at the leading edges. The laser Doppler velocimeter system used and the data reduction scheme employed are described in the report by Catalano et al.[15]

III. Experimental Results and Discussion

A. Mean Velocities

In Fig. 4, mean velocity profiles for the longitudinal component are presented for two downstream locations ($x/2r_0 = 2, 4$), and at one vertical position ($z/2r_0 = 0.5$) for all three flowfields. The ratio of the local excess velocity, $U - U_{FS}$, to the excess core velocity, $U_0 - U_{FS}$, is plotted vs lateral displacement (non-dimensionalized by twice the radius of the jet) from the centerline of the jet/flap assembly).

Initially, consider the comparison of the width of the three flow configurations. The freely expanding jet and the flow over the plate are quite comparable in width both at two and four diameters downstream. However, the flow over the flap has a large increase in width compared to the previous configurations at both downstream locations. Second, notice the effect of the confining walls on the decay of the centerline velocity. At $x/2r_0 = 4$, for example, the excess centerline velocity has decayed to approximately 0.95 ($U_0 - U_{FS}$) for the coflowing jet, 0.90 ($U_0 - U_{FS}$) for the plate configurations, and 0.55 ($U_0 - U_{FS}$) for the flow over the flap.

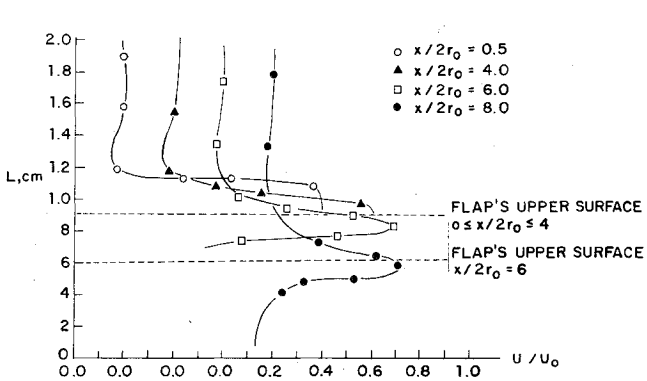

Fig. 3 Velocity surveys in test section, jet/flap configuration $y/2r_0 = 0$.

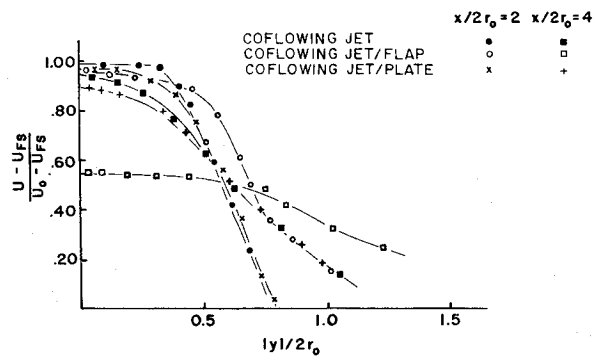

Fig. 4 Mean velocity profiles ($z/2r_0 = 0.5$).

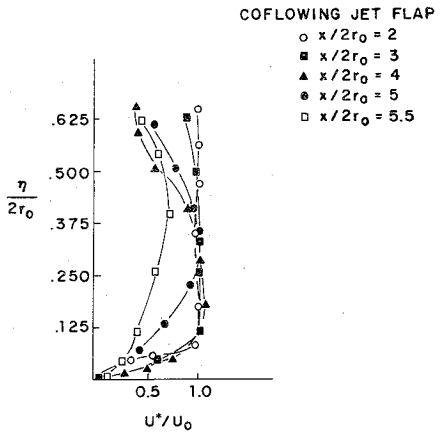

Fig. 5 Mean velocity profiles ($|y|/2r_0 = 0$).

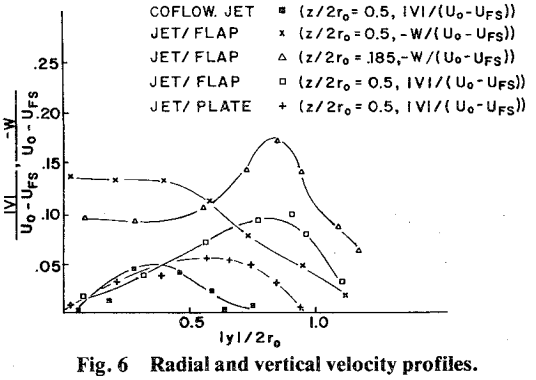

Fig. 6 Radial and vertical velocity profiles.

Thus, as the turbulent jet flows over the flap, the velocity field is significantly widened and decelerates much more rapidly.

Mean velocity parallel to the surface of the flap U^* vs perpendicular height above the surface of the flap η is presented in Fig. 5. An interesting observation that can be made concerning this series of profiles is that U^*/U_0 has a greater maximum value at $x/2r_0 = 4$ than at $x/2r_0 = 2$. This seems to indicate a net transfer of momentum from the core of the jet down toward the surface of the flap.

Mean velocities V were also measured in the lateral (y) direction for the unconfined jet, the flow over the plate, and the flap configuration at the same downstream location ($x/2r_0 = 4$ and $z/2r_0 = 0.5$). This comparison is presented in Fig. 6. It is interesting to observe that, for the flow over the flap, the maximum value of the ratio $V/(U_0 - U_{FS})$ has approximately doubled the maximum value found for the unconfined case.

For the flap configuration, a profile of the mean velocity W in the vertical direction z for the downstream location $x/2r_0 = 4$ and $z/2r_0 = 0.185$ also is presented in Fig. 6. Comparing this W profile with the one at $z/2r_0 = 0.5$ yields the observation that the jet seems to be rotating or rolling up as it spreads out over the surface of the flap. Whereas at $z/2r_0 = 0.5$, the maximum value of $W/(U_0 - U_{FS})$ is obtained at the centerline of the profile, for $z/2r_0 = 0.185$, this velocity ratio remains small and constant in the central region of the velocity field (i.e. $|y|/2r_0 = 0$) and reaches a maximum at approximately $|y|/2r_0 = 0.90$.

In Fig. 7, three vertical and three longitudinal mean velocity profiles are presented for various downstream locations ($x/2r_0 = 5.5$, 6.0, and 6.6) at the vertical position, $z/2r_0 = -0.57$ for the jet/flap configuration. These profiles indicate, in a quantitative as well as qualitative manner, the effectiveness of the flap in turning the flow. Figure 8 reinforces this by presenting a vectorial diagram of the resultant mean velocities at the centerline ($|y|/2r_0 = 0$) as the flow proceeds downstream.

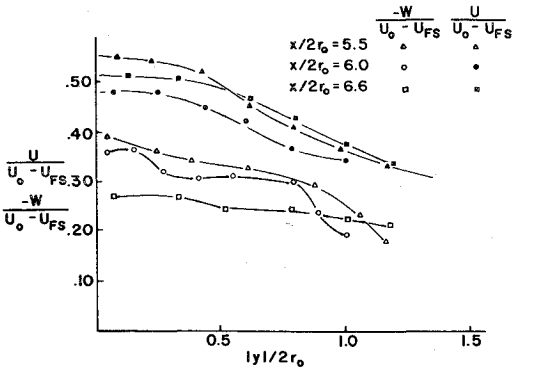

Fig. 7 Longitudinal and vertical velocity profiles ($z/2r_0 = -0.57$).

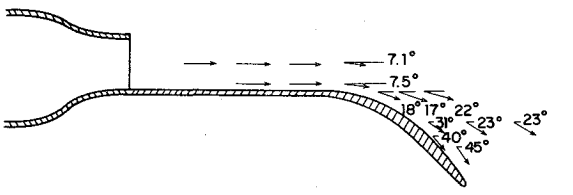

Fig. 8 Vectorial diagram of centerline mean velocities. (Scale: 0.33 in. = 20 m/sec.)

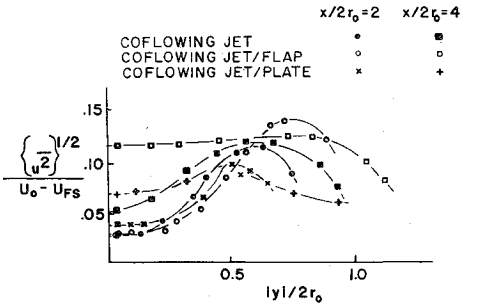

Fig. 9 Turbulent intensity profiles ($z/2r_0 = 0.5$).

B. Turbulent Intensities

Measuring turbulent fluctuations with an LDV setup is predicated on the fact that the marking particles can respond to the instantaneous flowfield For this experiment, particle lag at or near the exit plane of the nozzle is negligible. Also, the rms of the particle response differs from the fluid fluctuations rms by less than 2% up to approximately 2×10^3 Hz.[14] In effect, the particle behavior is similar to that of a low-pass filter, with the 3-dB point at 4×10^5 Hz.

The axial and lateral distributions of the turbulence intensities, $(\overline{u^2})/(U_0 - U_{FS})$, are plotted vs lateral displacement from the centerline at the vertical location, $z/2r_0 = 0.5$, in Fig. 9.

For the case of the unconfined coflowing jet, the turbulent intensity increases from about 2.5% to 5% at the centerline for the two downstream locations shown. In clear contrast to this case are the two confined flow configurations. Notice that for the flow over the plate, $(\overline{u^2})^{1/2}/(U_0 - U_{FS})$ is greater than either the unconfined or flap cases at $x/2r_0 = 2$. At $x/2r_0 = 4$, however, the flow over the flap clearly maintains the highest turbulent velocity level. In fact, $(\overline{u^2})^{1/2}/(U_0 - U_{FS})$ for the flow over the flap is more than five times the value it possessed at $x/2r_0 = 2$.

Another important observation concerns the relative turbulent intensity value of the three flow configurations in the region $0.5 \leq |y|/2r_0 \leq 1$. Whereas the flap seems to be amplifying the turbulence field in this region as well, the intensities of the plate flow are consistently lower than either of the other two cases. The presence of the confining straight

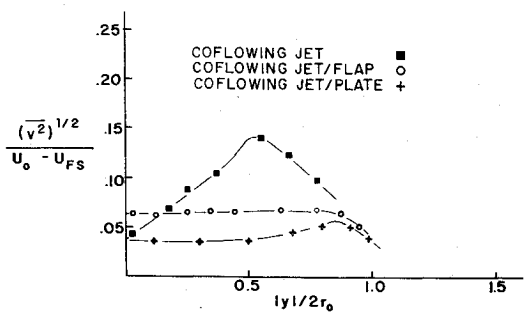

Fig. 10 Lateral turbulent intensity profiles ($x/2r_0=4$, and $z/2r_0=0.5$).

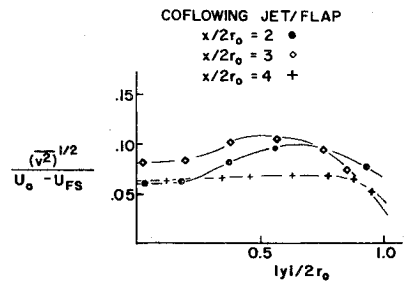

Fig. 11 Lateral turbulent intensity profiles for flap ($z/2r_0=0.5$).

wall seems to be diminishing the momentum transferring process occurring in the outer regions of the flow.

Turbulent intensities in the lateral direction, $(\overline{v^2})^{1/2}/(U_0-U_{FS})$, are shown in Figs. 10 and 11. In Fig. 10, a comparison of the intensities for the different flow configurations at the same downstream location ($x/2r_0=4$ and $z/2r_0=0.5$) is presented. Notice that the turbulent intensity in the lateral direction is much higher in the shearing layer of the unconfined jet than in either of the other two configurations. In Fig. 11 $(\overline{v^2})^{1/2}/(U_0-U_{FS})$ is presented for the flow over the flap. It indicates the change in the turbulence level as the flow reaches the curved portion of the flap structure.

C. Longitudinal Autocorrelations

The effects of the flap and the plate on the turbulent velocity field of the flow are shown clearly in a comparison of the autocorrelation coefficient curves. If $u=u(x,y,z,t)$ and $u'=(x+\Delta x,y,z,t)$ are the longitudinal fluctuating velocities at different downstream locations $(x,x+\Delta x)$ but at the same lateral and vertical positions (y,z) in the flow, then, at a given time, the correlation coefficient $R_{uu'}$ is defined by

$$R_{uu'}=\frac{\overline{uu'}}{(\overline{u^2})^{1/2}(\overline{u'^2})^{1/2}}$$

The autocorrelation coefficient R is given by

$$R=\frac{\overline{uu^*}}{(\overline{u^2})^{1/2}(\overline{u^{*2}})^{1/2}}$$

where $u^*=u(x,y,z,t+\Delta t)$. Autocorrelations can be converted to longitudinal correlations by using Taylor's hypothesis.[16] Autocorrelations of the axial velocity fluctuations were taken at the location $|y|/2r_0=0$ and $|y|/2r_0=0.5$ at the vertical position, $z/2r_0=0.5$, for $x/2r_0=2$ and 4 in all three flowfields. In Fig. 12 the curves are presented for the transverse location $|y|/2r_0=0$ for both the unconfined jet and the flow over the flap. Notice that for the unconfined jet, the autocorrelation coefficient has a damped sinusoidal behavior about the value $R=0.0$ at both $x/2r_0=2$ and $x/2r_0=4$. This is characteristic of the autocorrelation coefficient in the potential core region of the jet. With the flap in the flow, however, this sinusoidal nature first is reduced at $x/2r_0=2$ and then is eliminated by $x/2r_0=4$. This is consistent with the rapid increase in the turbulence in what was the potential core

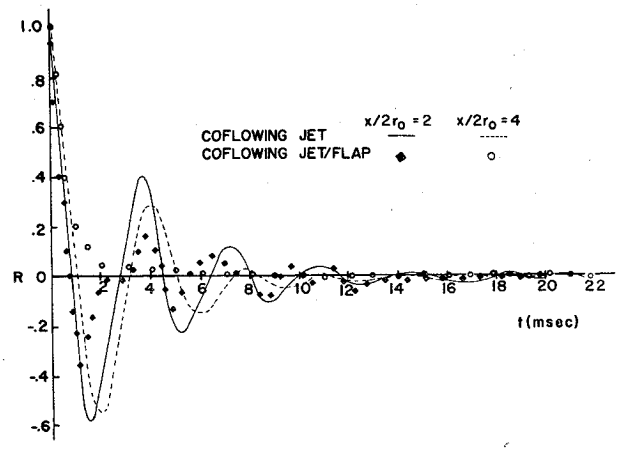

Fig. 12 Longitudinal autocorrelations ($z/2r_0=0.5$).

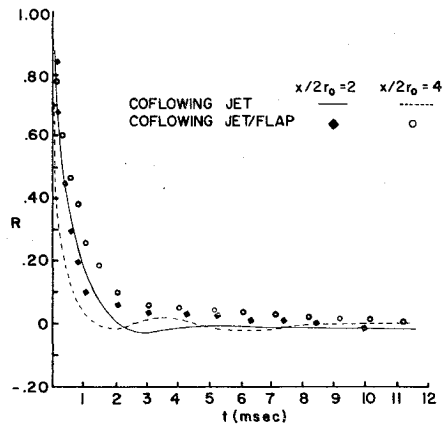

Fig. 13 Longitudinal autocorrelations ($z/2r_0=0.5$).

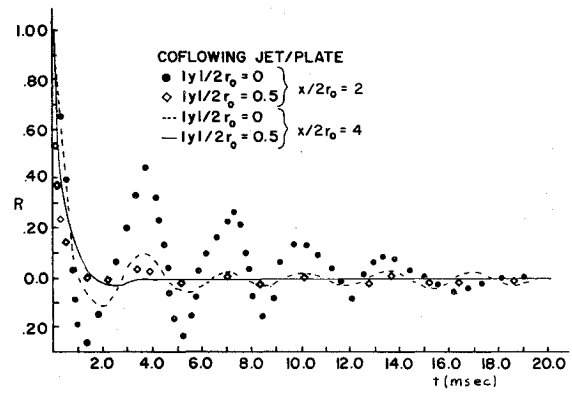

Fig. 14 Longitudinal autocorrelations for flow over plate ($z/2r_0=0.5$).

region. The increase in the turbulence level masks out the smaller pressure fluctuations in the core which are caused by the passing of vortices. In Fig. 13 autocorrelation coefficients are presented for the lateral location $|y|/2r_0=0.5$. Notice that there is little difference in curves for the unconfined jet or the flow over a flap. Since the location of the measurement is in the mixing region for both flowfields, the turbulence is quite high and masks out the smaller pressure fluctuations.

Turning next to a discussion of the effects of the plate on the turbulence of the jet, longitudinal autocorrelations are presented in Fig. 14. For the curves corresponding to the centerline ($|y|/2r_0=0$), the correlation looks very similar to those determined for the unconfined jet. At $x/2r_0=4$, unlike the case for the flow of the flap, the curve still has a damped sinusoidal nature. Out in the mixing region of the flow ([$|y|$/

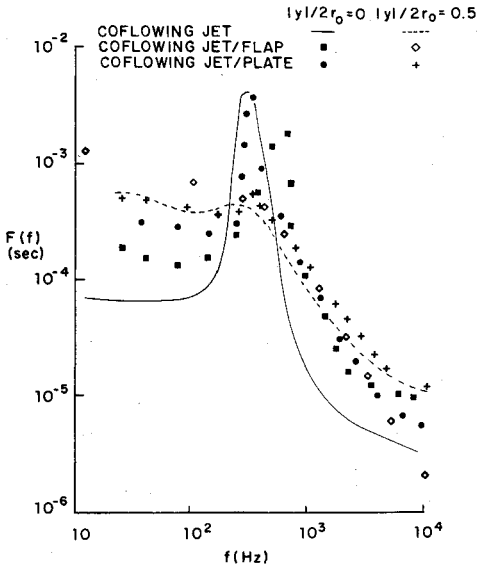

Fig. 15 Spectral density curves ($x/2r_0 = 2$, $z/2r_0 = 0.5$).

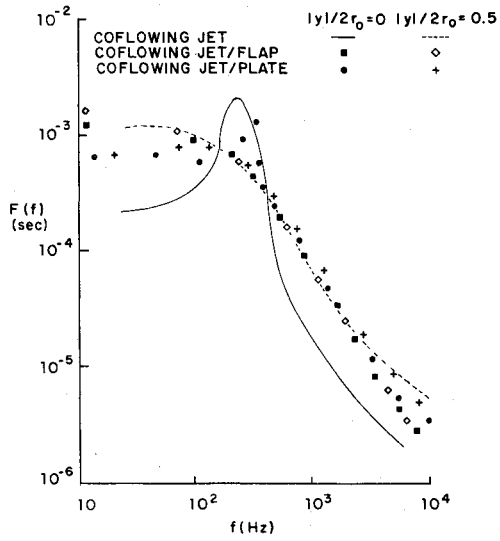

Fig. 16 Spectral density curves ($x/2r_0 = 4$, $z/2r_0 = 0.5$).

$2r_0 = 0.5$), the higher turbulence level again masks out the smaller pressure disturbances.

To determine the spectral density curves, a computer program is used which takes the Fourier Transform of the autocorrelation functions. These are presented for $x/2r_0 = 2$ (Fig. 15) and $x/2r_0 = 4$ (Fig. 16), at the vertical location $z/2r_0 = 0.5$. The profiles are normalized so that the area underneath each curve is 1.00.

Focusing initially on the unconfined coflowing jet, the power spectrum in the potential core ($|y|/2r_0 = 0$) is characterized by a large "bump" or peak.[17,18] The peak is quite pronounced at $x/2r_0 = 2$ (Fig. 15) whereas it is slightly attenuated and shifted to a higher frequency at $x/2r_0 = 4$ (Fig. 16). Next, consider the effects of the plate on the turbulent flowfield. At $x/2r_0 = 2$ (Fig. 15), the characteristic peak has approximately the same magnitude as the unconfined flow but with a slight shift in frequency. At $x/2r_0 = 4$ (Fig. 16), the peak is still present though with a smaller magnitude than the unconfined jet and at a slightly higher frequency. Contrasting the aforementioned configurations to the flow over the flap is quite instructive. At $x/2r_0 = 2$ (Fig. 15), the peak has been diminished markedly and shifted to a higher frequency than before. Following the flow downstream, at $x/2r_0 = 4$ (Fig. 16), notice that the characteristic peak is totally absent.

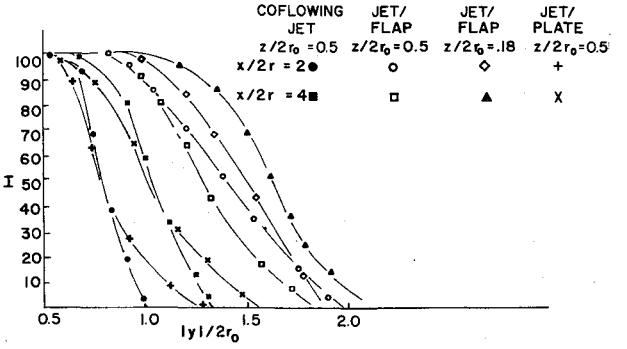

Fig. 17 Intermittency profiles.

In the shearing layer between the faster moving jet and the slower moving outer flow, the distinctions that were possible to make before among the three configurations are no longer realizable. In this region, the peak virtually is masked out entirely by the relatively high turbulence levels.

D. Intermittency

The probability of the occurrence of turbulence at any point within the flowfield is called the intermittency factor (I). Profiles for intermittency are presented for the region outside the lip of the jet. The radial and axial distributions of the intermittency factor at various vertical locations for the unconfined jet and flows over the flap and plate are given in Fig. 17. For the vertical location $z/2r_0 = 0.5$, the intermittency flowfield with the flap in place is significantly wider than either the unconfined or plate case, but actually decreases in width as the jet progresses downstream. For the vertical position $z/2r_0 = 0.180$, the intermittency flowfield width with the flap present is greater than at $z/2r_0 = 0.5$, and it also increases in size as the jet progresses downstream. Thus, the flap acts to draw the jet down toward the surface and to increase the flowfield's width. The flap serves to transform what was an axisymmetric jet into a flow with a rather elongated oval-type cross section.

Compare the behavior of the intermittancy field to that of the velocity field at $x/2r_0 = 0.5$ for the flow over the flap. The flap serves to increase the intermittency field quite rapidly initially, as has been stated previously. With respect to the velocity field, the flap again serves to increase the width but not nearly as soon downstream nor at such a rapid rate. Thus, the behavior of the intermittency field seems to be ahead of the development of the velocity field.

IV. Summary

An experimental investigation of the effects of confining surfaces on an axisymmetric coflowing turbulent jet was made. Mean velocities, turbulent intensities, velocity autocorrelations and power spectral densities, and intermittencies were determined. Comparison among measurements of quantities at the same location in the flowfield for the three different configurations were made. The following results were obtained.

1) The intermittency and velocity field widths were increased markedly by the presence of the flap. The intermittency field increased in width close to the upper surface of the flap ($z/2r_0 = 0.180$) as the flow progressed downstream, whereas this was not the case one radius above the structure ($z/2r_0 = 0.5$). In contrast to this is the behavior of the velocity field width at $z/2r_0 = 0.5$, for it actually increases in size as the flow progresses downstream. The velocity field width seemed to be lagging behind the behavior of the intermittency field.

2) The excess mean velocity at the centerline of the jet/flap flowfield experiences the largest deceleration. At $x/2r_0 = 4$, the excess centerline velocity has decayed to 0.55 – its exit

plane value. At the same position relative to the nozzle, the excess centerline velocity has decayed to 0.90 $(U_0 - U_{FS})$ for the flow over the plate and $0.95(U_0 - U_{FS})$ for the unconfined jet.

3) The vertically traversed profiles of U^*/U_0 vs η/r_0 indicate that there was a net transfer of momentum from the central part of the jet down toward the surface of the flap. A greater maximum velocity was achieved for the profile at $x/2r_0 = 4$ than at $x/2r_0 = 2$.

4) The flap has the greatest effect on the turbulent structure of the coflowing jet. The curved wall surface served to break up the potential core region of the jet with its relatively low turbulence level much more quickly than was the case for either the unconfined flow or the flow over the plate. The turbulent intensities increased at a much more rapid rate for the first several diameters downstream. Also, the autocorrelation coefficient curves lost their dominant frequency character, and the "bump" or peak in the power spectrum in what was the potential core region was initially diminished and eventually masked out completely by the higher turbulence level much more quickly for the flow over the flap than in either of the other two cases.

5) Measurement of the velocity in the vertical direction over the surface of the flap indicated that the flow seems to be revolving or rolling up as it spreads out over the curved wall.

Acknowledgment

This work was supported in part by NASA Grant No. NGR 47-005-219 and by NSF Grant No. ENGR 75-22488.

References

[1] Catalano, G.D., Morton, J.B., and Humphris, R.R., "An Experimental Investigation of an Axisymmetric Jet in a Coflowing Airstream," *AIAA Journal,* Vol. 14, Sept. 1976, pp. 1157-1158.

[2] Schoenster, J.A., Willis, C.M., Schroeder, J.C., and Mixson, J.S., "Acoustic-Loads Research for Powered Lift Configurations," *Powered-Lift Aerodynamics and Acoustic Conference,* May 24-26, 1976, Langley Research Center, Hampton, Va., pp. 429-444.

[3] Hari, V., "A Method to Analyze the Wall Jet Flow," *Aeronautical Journal,* Vol. 77, Oct. 1973, pp. 512-515.

[4] Forthman, E., "Turbulent Jet Expansion," NACA TM 789, March 1936.

[5] Glauert, M.B., "The Wall Jet," *Journal of Fluid Mechanics,* Vol. 1, April 1956, pp. 625-643.

[6] Schwarz, W.H. and Cosart, W.P., "The Two-Dimensional Turbulent Wall Jet," *Journal of Fluid Mechanics,* Vol. 10, March 1961, pp. 481-495.

[7] Sigalla, A., "Measurements of Skin Friction in a Plane Turbulent Jet," *The Aeronautical Journal of the Royal Aeronautical Society,* England, Vol. 62, Dec. 1958, pp. 873-878.

[8] Myers, G.E., Schauer, J.J., and Eustis, R.H., "The Plane Turbulent Wall Jet, Part 1, Jet Development and Friction Factor," Mechanical Engineering Department, Stanford University, Stanford, Calif., TR No. 1, June, 1961.

[9] Dvorak, F.A., "Calculation of Turbulent Boundary Layers and Wall Jets over Curved Surfaces," *AIAA Journal,* Vol. 11, April 1973, pp. 517-524.

[10] Blackwelder, R.F. and Koavaznay, L.S.G., "Time Scales and Correlations in a Turbulent Boundary Layer," *The Physics of Fluids,* Vol. 15, Sept. 1972, pp. 1545-1554.

[11] Rajaratnam, N. and Pani, B.S., "Three-Dimensional Turbulent Wall Jets," *Journal of the Hydraulics Division, ASME Transactions,* Vol. 100, HY 1, Jan. 1974, pp. 69-83.

[12] Narain, J.P., "Three Dimensional Turbulent Wall Jets," *The Canadian Journal of Chemical Engineering,* Vol. 53, June 1975, pp. 245-251.

[13] Hill, P.G., "Turbulent Jets in Ducted Streams," *Journal of Fluid Mechanics,* Vol. 22, Jan. 1965, pp. 161-186.

[14] Haertig, J., "Introductory Lecture on Particle Behavior," *Proceedings of the ISL/AGARD Workshop on Laser Anemometry,* May 5-7, 1976, German-French Research Institute, St. Louis, France, pp. 1-40.

[15] Catalano, G.D., Morton J.B., and Humphris, R.R., "An Experimental Investigation of an Axisymmetric Jet in a Coflowing Airstream," NASA CR 143104 (N76-26425), 1976.

[16] Tennekes, H. and Lumley, J.L., *A First Course in Turbulence,* MIT Press, Cambridge, Mass., 1972.

[17] Bradshaw, P., Fevis, D.H., and Johnson, R.J., "Turbulence in Noise Producing Region of Circular Jets," *Journal of Fluid Mechanics,* Vol. 19, Aug. 1964, pp. 591-624.

[18] Ko, N.W.U. and Davies, P.O.A.L., "The Near Field Within the Potential Core of Subsonic Cold Jets," *Journal of Fluid Mechanics,* Vol. 50, 1971, pp. 49-78.